Ceramics-Silikáty 67 (2), 167-173 (2023)
www.ceramics-silikaty.cz doi: 10.13168/cs.2023.0014

HYDRATION AND EARLY MECHANICAL PERFORMANCE OF BELITE SULFOALUMINATE CEMENT CONTAINING $MgAl_2O_4$ FROM SOLID WASTE

ZENGYAO WANG*, HAO LIU**, LIANG YU*, JINGHUA YAN*, FENGNIAN WU*, #SHOUDE WANG*, #PIQI ZHAO*, XIN CHENG*

*Shandong Provincial Key Laboratory of Preparation and Measurement of Building Materials, University of Jinan, Jinan 250022, China
**China Railway Construction Group Co., Ltd. Shandong Branch, Jinan 266109, China

#E-mail: 401795556@qq.com, mse_zhaopq@ujn.edu.cn

Submitted February 20, 2023; accepted March 27, 2023

Keywords: Belite sulfoaluminate cement, $MgAl_2O_4$, Calcination, Setting time, Hydration, Compressive strength

This study dealt with the use of gold tailings, red mud, bauxite, desulfurised gypsum and high magnesium limestone as the raw materials in the production of a belite sulfoaluminate cement clinker containing $MgAl_2O_4$. The hydration and early mechanical properties of this cement were characterised by isothermal calorimetry, a mechanical test, X-ray diffraction and a thermal analysis. The results showed that the optimal calcination temperature to obtain a satisfactory clinker strength was 1350 °C and the corresponding 1, 3 and 7-day strengths were 27.7, 45.8 and 54.3 MPa, respectively. The initial and final setting times of the cements range between 20 and 31 minutes. The cements had the characteristics of rapid hardening and the main hydration products were AFt, AFm and AH_3. The total hydration heat release of this cement within the first 50 hours was only 158 $J\cdot g^{-1}$, which could effectively avoid the generation of internal cracks in the cement and has the potential to be applied to large concrete projects. Furthermore, the $MgAl_2O_4$ mineral phase was inert in the belite sulfoaluminate cement and did not participate in the hydration reaction, which eliminates the disadvantage of MgO in the cement systems and potentially increases the use of high magnesium limestone in cement production.

INTRODUCTION

The production of Portland Cement consumes large amounts of energy, because the high calcium phases in the clinker are required to be formed at a high sintering temperature of about 1450 °C [1-4]. In addition, the calcination of limestone produces huge quantities of CO_2 during the production of Portland cement which responsible for 6–7 % of the total world CO_2 emissions [1, 5, 6]. In order to reduce energy consumption and CO_2 emissions, interest has been registered in producing different green low-carbon cements. Belite sulfoaluminate cement (B-CSA) is a hydraulic cementitious material with ye'elimite ($C_4A_3\$$) and belite (β-C_2S) as the main clinker mineral phases [7, 8]. Compared to ordinary Portland cement (OPC), the most significant advantage of B-CSA cement is the reduction of the calcination temperature and CO_2 emissions in the clinker sintering [9-14]. B-CSA cement also has excellent properties, such as rapid hydration, high early strength, low volume shrinkage and sulfate corrosion resistance [15-18], and it is widely used in marine engineering, permeability resistance engineering and emergency repair works, etc. [5, 13].

China generates a large amount of industrial solid waste every year, which not only occupies land resources, but also poses serious environmental and safety hazards [19-21]. However, the industrial solid waste, which must be eliminated, can also be considered as a source of energy, provided that they can be recovered in a reasonable way [20]. The raw materials for the production of B-CSA cement can be replaced by solid waste [5,17], such as fly ash [22], red mud [23, 24], gypsum [25], slag [26] and other waste materials. Recent studies conducted by researchers have demonstrated the feasibility of producing B-CSA cement from industrial solid waste as the raw material. Gao et al. [5] successfully synthesised belite-rich sulfoaluminate cement (SAC) by using industrial solid waste (Bayer red mud, blast furnace slag, steel slag, flue gas desulfurisation and carbide slag) and the synthetic cement had excellent hydration performance in the early stage and could be used as a repair material. A. Rungchet et al. [27] prepared sulfoaluminate-belite cement using industrial waste, such as bag house dust, low-calcium fly ash and scrubber sludge, which had hydration properties comparable to those of Ordinary Portland Cement. Yan et al. [28] produced belite sulfoaluminate-ternesite cements by using phosphogypsum, achieving the coexistence of ye'elimite and ternesite where the hydration of ternesite significantly increased the late strength of the cement. The synthetic belite sulfoaluminate cement [18] from petroleum coke desulfurisation residue (PCDR), fly ash (FA), carbide slag (CS) and bauxite (BX) has excellent performance with a compressive strength of 51.4 MPa at 28 d of hydration. The industrial solid waste can use up to 80 % of the hydration and the cumulative heat release of the developed cement (191 $J \cdot g^{-1}$) at 72 h was lower than that of SAC (198 $J \cdot g^{-1}$).

Based on the above information, this work prepared belite sulfoaluminate cement containing $MgAl_2O_4$ (named as HB$AC) from industrial solid waste as the raw material. The early hydration behaviour and mechanical performance of the HB$AC cement were investigated, and the stability of $MgAl_2O_4$ during hydration was also discussed.

EXPERIMENTAL

Materials

The raw materials adopted in this experiment were gold tailing (GT), red mud (RM), high magnesium limestone (HML), desulfurisation gypsum (DG) and low-grade bauxite (BX). The chemical compositions of the raw materials were determined by X-ray fluorescence (XRF) and are shown in Table 1. The design of the HB$AC cement clinker with different calcium sulfoaluminate (C_4A_3\$) ratios is shown in Table 2.

Table 1. The chemical compositions (wt. %) of the raw materials.

Chemical composition	GT	RM	HML	DG	BX
CaO	2.58	3.33	47.52	32.41	8.10
SiO_2	62.28	15.60	4.62	2.11	7.18
Al_2O_3	17.52	22.40	1.34	0.80	58.99
MgO	1.15	0.18	3.86	0.83	0.22
SO_3	1.18	0.31	0.06	40.63	2.42
Fe_2O_3	2.54	26.62	0.57	0.34	1.83
NaO	2.55	12.89	0	0.15	0.10
K_2O	4.25	0.07	0.32	0.11	0.68
LOI	3.16	11.23	41.72	21.87	41.38

Table 2. Design of the raw mixtures with different oxide compositions.

Group	C_4A_3\$ content (%)	Oxide ratio (wt. %)					
		CaO	SiO_2	Al_2O_3	SO_3	Fe_2O_3	MgO
A	40	46.81	14.50	22.46	7.57	3.04	3.63
B	35	48.04	16.09	18.12	6.95	3.04	3.80
C	30	49.27	17.67	15.78	6.33	3.03	3.97
D	25	50.50	19.24	13.45	5.72	3.03	4.15
E	20	51.72	20.81	11.13	5.11	3.02	4.32

Synthesis of the clinker

According to the design ratio, the pressed raw mixtures were sintered at 1350 °C for 75 min and then cooled rapidly in air to obtain the clinker. The clinker was sufficiently ground and sifted through 150 meshes and mixed well at a ratio of 85 %:15 % clinker to gypsum to obtain a belite sulfoaluminate cement containing $MgAl_2O_4$ at the target mineral ratio, the density and specific surface area of the obtained cement clinker by testing are shown in Table 3.

Table 3. Density and specific surface area of the HB$AC cements with the different oxide compositions.

Group	Density ($g \cdot cm^{-3}$)	Specific surface area ($m^2 \cdot kg^{-1}$)
A	2985	448
B	2995	443
C	2974	452
D	2993	442
E	2976	447

Testing methods

Setting time

The setting time of the HB$AC cement paste was determined by a manual Vicat apparatus, as described in the Chinese standard GB/T 1346–2001 (China).

Compressive strength

An MTS (MTSCMT5504, China) testing machine was used to test the compressive strength of the specimens with displacement control at a speed of 2.0 $mm \cdot min^{-1}$. The average value and standard deviation were taken by six specimen tests for each group.

Isothermal calorimetry

An eight-channel TAM AIR calorimeter was employed to monitor the heat evolution of the cement hydration. The w/s ratio was maintained at 0.40 for all the measurements.

XRD and TG-DTA analysis

A Bruker D8A25 X-ray diffractometer (XRD) was used to observe the phase composition of the specimens. The XRD data were collected from 5° to 60° under CuKα radiation with a voltage of 40 kV and a current of 40 mA. The thermal decomposition processes that occurred in the hydrated specimens were characterised a Mettler Toledo TGA/DSCI (thermogravimetric analyser-differential scanning calorimetry instrument) with a heating rate of 10 $°C \cdot min^{-1}$ from 30 to 1000 °C in the N_2 atmosphere. The derivative thermogravimetry (DTG) data was collected by the first derivative of the weight curve.

RESULTS AND DISCUSSION

Setting time

Figure 1 shows the setting time of the HB\$AC cement paste. The results show that the initial and final setting times of HB\$AC cement paste were close, which was related to the rapid hardening of the HB\$AC cement. The time between the initial and final set was between 20 and 31 minutes for all the pastes and when decreasing the $C_4A_3\$$ content, the setting times for the HB\$AC cement paste increased. The initial setting time of group A was 5 minutes shorter than group E (22 min → 27 min) because the $C_4A_3\$$ content in group A was higher than in group E. The hydration rate of $C_4A_3\$$ was fast and a large number of hydration products were produced after contact with water [29], which allowed the crystals to overlap easily, resulting in the rapid setting and hardening of the HB\$AC cement paste. When the $C_4A_3\$$ content was decreased from 40 to 20 wt. %, the time to final set for HB\$AC cement paste was increased by approximately 9 minutes (+40.9 %). In addition, the water requirement of the standard consistency of the cement did not appear to be significantly affected by the $C_4A_3\$$ content and the values for the five groups of HB\$AC cement were around 30 %.

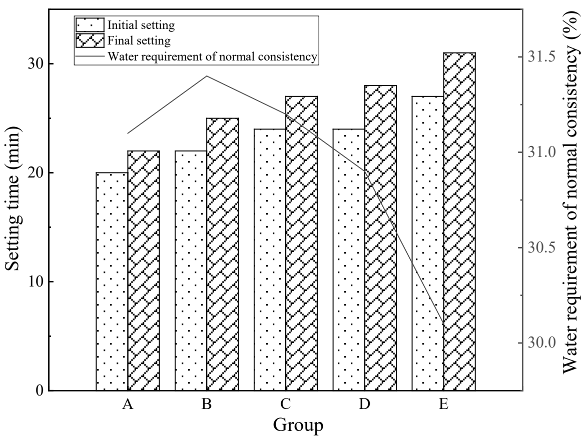

Figure 1. Setting time of the HB\$AC cement paste with the varying $C_4A_3\$$ contents.

Compressive strength

The compressive strength of the HB\$AC cement is an important indicator to evaluate whether or not if it can be applied to concrete construction projects. Figure 4 shows the results of the compressive strength of the cement specimens at different curing times. It can be seen from Figure 2 that the Group A cement showed higher compressive strengths than the Group C and Group E cement pastes at any hydration time. The compressive strengths of Group A at 1 d, 3 d and 7 d were 27.1, 43.73 and 53.36 MPa, respectively. Compared with Group C and Group E, the early strength of Group A developed rapidly and the 1 d compressive strength was 27.1 MPa. This may be related to the rapid hydration of $C_4A_3\$$, which can react with calcium sulfate when dissolved rapidly in water to form ettringite, thus contributing to the early strength development of the HB\$AC cements. After 7 days of hardening, the compressive strengths of Group A exhibited a significant increase [27, 28, 30].

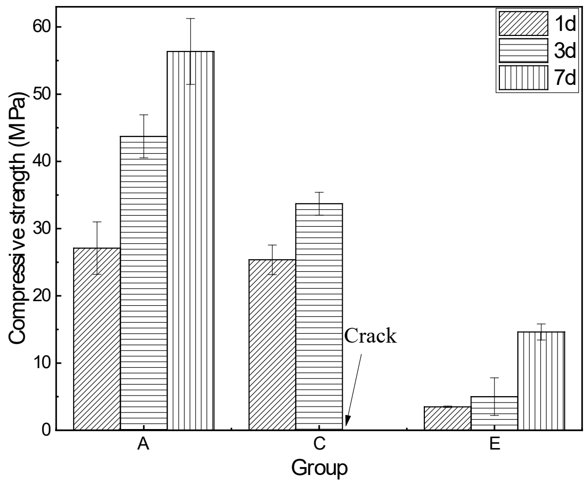

Figure 2. Compressive strength of the HB\$AC cement in the different groups.

When cured for 7 days, cracks appeared in the Group C specimens. The main reason for the cracking was the long-term calcination increased the CaO content derived from the decomposition of gypsum, in which the hydration formed the $Ca(OH)_2$ causing the volume expansion and cracking of the cement paste. The compressive strength of Group E showed slow development, and the strength increased by 11.13 MPa from day 1 to day 7. Although the compressive strength of Group E increased, it is still low, with a 7-day compressive strength of only 14.63 MPa. This was due to the low $C_4A_3\$$ content of Group E, in which the hydration provides insufficient strength development. Although Group E has a high C_2S content, the slow hydration was not conducive to the development of the 7-day strength. These results suggest that the higher the $C_4A_3\$$ content, the higher the early strength and the faster the later strength development of the HB\$AC cements.

In order to verify the optimum temperature of the calcination process, the compressive strength of the Group A cement clinker with the best mechanical properties was tested at different temperatures. As shown in Figure 3, the compressive strength of the specimens increased gradually when increasing the calcination temperature from 1200 to 1350 °C. When the calcination temperature was 1350 °C, the cement clinker showed the highest $C_4A_3\$$ content, which contributed to the early

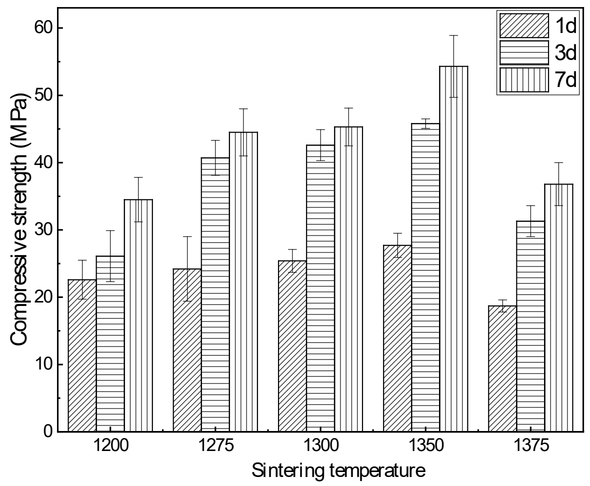

Figure 3. Influence of the sintering temperature on the compressive strength of the specimens.

strength. The development of the mechanical properties of the cement was limited by the small amount of mineral phases in the clinker which were produced at a lower calcination temperature. The 7-day compressive strength of HB$AC sintered at 1375 °C was decreased by about 32.2 % compared to HB$AC obtained at 1350 °C.

Hydration characteristics

With regards to the hydration heat analysis of the sintered clinker with the different $C_4A_3\$$ contents, it was important to study the hydration rate and reaction degree of the HB$AC cement. The heat evolutions of three groups of cements (A, C and E) at a w/c of 0.4 that were investigated using an isothermal conduction calorimeter are presented in Figure 4 and Figure 5. Figure 4 shows that the hydration rate of Group A was the fastest, successively followed by Group C and Group E. This showed that the high $C_4A_3\$$ content accelerated the hydration process of the HB$AC cement, thus reducing the setting time and enhancing the early mechanical properties. In the early stage of hydration, the reaction was very rapid, the initial dissolution reaction of the $C_4A_3\$$ minerals occurs between 0.5 and 12 min and the appearance of the first exothermic peak may also be associated to the rapid reaction of the f-CaO contained in the HB$AC clinker with water [12, 18]. Then, the reaction rate becomes quite slow and enters the induction period. At the end of the induction period, the hydration is accelerated again. In the acceleration phase, the exothermic rate of hydration gradually increased, the second exothermic heat peak appeared in 50–200 min, which was mainly caused by the reaction between the calcium sulfate and $C_4A_3\$$ to form ettringite and AH_3 [31]. The subsequent hydration rate gradually decreases with an increase in time, the exothermic rate slowed down until the end of the hydration process [32].

Figure 5 shows the cumulative heat release of the three groups of cements. The bulk of all the specimens' total heat (> 80 %) evolved within the first 20 hours. There was a significant difference in the total heat release of hydration between the three groups of cements. With an increase in the $C_4A_3\$$ hydration degree, the cumulative heats of Group A and Group C were 197 and 171 $J \cdot g^{-1}$, respectively, after 50 hours of hydration, while the total heat release of Group E was only 70 $J \cdot g^{-1}$, indicating that the slow hydration reaction rate of Group E. As the total heat of the Group A specimens was below 200 $J \cdot g^{-1}$, the HB$AC cement which was composed of a high $C_4A_3\$$ content had a low hydration heat characteristic and can be expected to be used in large concrete construction projects.

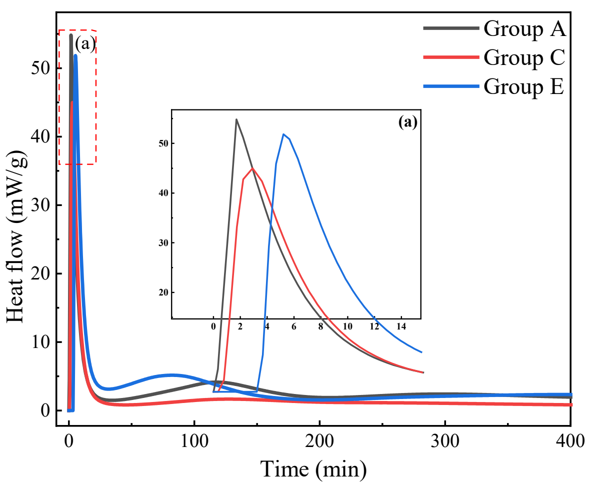

Figure 4. Heat of the hydration of the HB$AC cement with the varying $C_4A_3\$$ contents.

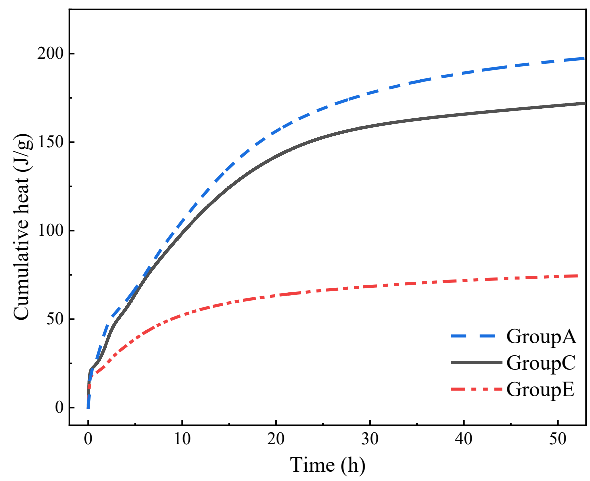

Figure 5. Cumulative heat of the HB$AC cement with the varying $C_4A_3\$$ contents.

X-ray diffraction analyses were carried out to identify the hydration products in the HB\$AC cement. As shown in Figure 6, the hydration products of HB\$AC were mainly composed of ettringite (AFt), monosulfoaluminate (AFm), unhydrated C_2S, unhydrated gypsum and the inactive mineral $MgAl_2O_4$. When increasing the curing time, the ettringite content increases, while the diffraction peak of gypsum decreases in intensity. The formation of ettringite was due to the reaction of $C_4A_3\$$ with gypsum and water. A significant amount of belite was still present after 7 days of cement hydration, which was beneficial to the later strength development of the slurry, since most of the hydration of C_2S occurred after 28 days [5]. It is worth noting that the diffraction peaks of $MgAl_2O_4$ did not change significantly with the age of hydration, which indicates that $MgAl_2O_4$ was inert and not involved in the hydration reaction. The MgO was effectively solidified, which is conducive to increasing the use of high magnesium limestone in cement production.

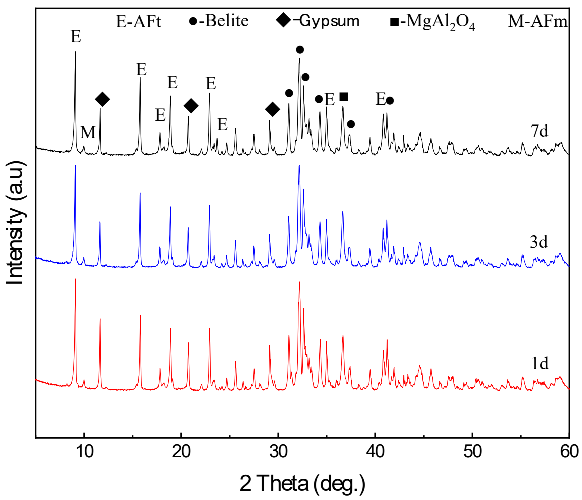

Figure 6. XRD patterns of the HB\$AC cement hydrated for 1, 3 and 7 days.

To further demonstrate the change in the hydration products of the HB\$AC cement with hydration age, a thermal analysis was carried out on the Group A cement specimens of different ages and the TG-DSC results for the cement slurry are shown in Figure 7. After 1 day of hydration, the endothermic peak of gypsum ($CaSO_4 \cdot 2H_2O$) and ettringite (AFt) appeared in the temperature range of 75 to 150 °C, which was consistent with the results of the XRD analysis. The peak centred at approximately 280 °C showed aluminium hydroxide (AH_3) presented in the specimen. Compared with the specimens at different ages of hydration, it was found that with an increase in the hydration time, the peak area of the first endothermic peak became smaller, and the area was close to 0 after 7 days of hydration, which indicated that a large amount of gypsum ($CaSO_4 \cdot 2H_2O$) participated in the hydration reaction. The amount of monosulfoaluminate (AFm) gradually increased as the age of the conservation increased, which was due to the conversion of the AFt product to AFm by the desulfurisation reaction. In addition, there was no obvious C-S-H peak on the TG-DTG curve. This is due to the fact that the C_2S was not yet fully hydrated.

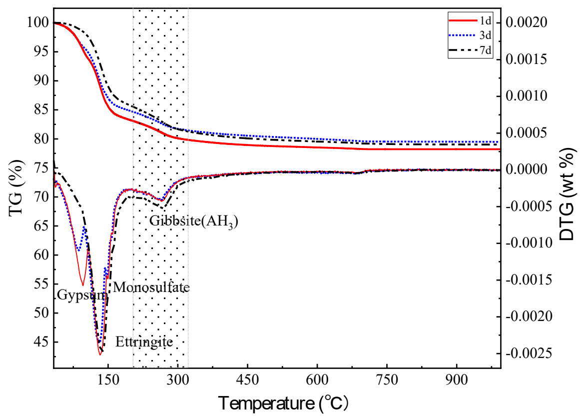

Figure 7. TG-DTG curve of the HB\$AC cement with the 40 % $C_4A_3\$$ content (1, 3 and 7 days).

CONCLUSIONS

The following conclusions were drawn from the present study.

(1) The initial and final setting times of HB\$AC cements were similar, between 20 and 31 minutes, showing that HB\$AC cements had the characteristics of rapid hardening. The water requirement for the standard consistency of the HB\$AC cements were around 30 %.

(2) Increasing the $C_4A_3\$$ content in the cement clinker improved the compressive strength, which was related to the reaction of $C_4A_3\$$ and gypsum to form ettringite. The HB\$AC clinkers had the optimal mechanical properties at a calcination temperature of 1350 °C and the corresponding compressive strengths at 1, 3 and 7 days were 27.7, 45.8 and 54.3 MPa, respectively.

(3) The HB\$AC cement composed of a high content of $C_4A_3\$$ had a low hydration heat characteristic. The total exothermic heat of the hydration at 50 hours was only 158 $J \cdot g^{-1}$, which could effectively reduce the generation of cement cracks and is expected to be applied in large concrete structures.

(4) The early hydration products of the HB\$AC cement were mainly composed of AFt, AFm, and AH_3. The $MgAl_2O_4$ in the cement clinker was inert and not involved in the hydration reaction, which is conducive to eliminating the disadvantage of MgO in the cement systems and improving the consumption of low-grade high magnesium limestone in cement production.

Acknowledgements

This work was supported by the National Key Research and Development Plan of China (No. 2021YFB3802002), Natural Science Foundations of China (52072149), Natural Science Foundations of China-Shandong Joint Fund (U22A20126).

REFERENCES

1. Ashraf W., Olek J. (2016): Carbonation behavior of hydraulic and non-hydraulic calcium silicates: potential of utilizing low-lime calcium silicates in cement-based materials. *Journal of Materials Science, 51*, 6173-6191. Doi: 10.1007/S10853-016-9909-4/figures/22
2. Huntzinger D. N., Eatmon T. D. (2009): A life-cycle assessment of Portland cement manufacturing: comparing the traditional process with alternative technologies. *Journal of Cleaner Production, 17*(7), 668-675. Doi: 10.1016/j.jclepro.2008.04.007
3. Popescu C. D., Muntean M., Sharp J. H. (2003): Industrial trial production of low energy belite cement. *Cement and concrete Composites, 25*(7), 689-693. Doi: 10.1016/S0958-9465(02)00097-5
4. Schneider M., Romer M., Tschudin M., Bolio H. (2011): Sustainable cement production—present and future. *Cement and Concrete Research, 41*(7), 642-650. Doi: 10.1016/j.cemconres.2011.03.019
5. Gao Y., Li Z., Zhang J., Zhang Q., Wang Y. (2020): Synergistic use of industrial solid wastes to prepare belite-rich sulphoaluminate cement and its feasibility use in repairing materials. *Construction and Building Materials, 264*, 120201. Doi: 10.1016/j.conbuildmat.2020.120201
6. Schneider M. (2019): The cement industry on the way to a low-carbon future. *Cement and Concrete Research, 124*, 105792. Doi: 10.1016/j.cemconres.2019.105792
7. Juenger M. C. G., Winnefeld F., Provis J. L., Ideker J. H. (2011): Advances in alternative cementitious binders. *Cement and Concrete Research, 41*(12), 1232-1243. Doi: 10.1016/j.cemconres.2010.11.012
8. Burris L. E., Kurtis K. E. (2022): Water-to-cement ratio of calcium sulfoaluminate belite cements: Hydration, setting time, and strength development. *Cement, 8*, 100032. Doi: 10.1016/j.cement.2022.100032
9. Zhang T., Yu Q., Wei J., Zhang P., Chen P. (2011): A gap-graded particle size distribution for blended cements: analytical approach and experimental validation. *Powder technology, 214*(2), 259-268. Doi: 10.1016/j.powtec.2011.08.018
10. Li R., Zhang J., He W., Nie D., Zhang Y. (2023): Preparation of belite-sulfoaluminate cement with phosphate-rock acid-insoluble residue: Modification and influence of impurity ions on cement properties. *Construction and Building Materials, 365*, 130077. Doi: 10.1016/j.conbuildmat.2022.130077
11. Žibret L., Ipavec A., Dolenec S. (2022): Microstructural characteristics of belite–sulfoaluminate cement clinkers with bottom ash. *Construction and Building Materials, 321*, 126289. Doi: 10.1016/j.conbuildmat.2021.126289
12. He W., Li R., Nie D., Zhang J., Wang Y., Zhang Y., Chen Q. (2022): Belite-calcium sulphoaluminate cement prepared by EMR and BS: Hydration characteristics and microstructure evolution behavior. *Construction and Building Materials, 333*, 127415. Doi: 10.1016/j.conbuildmat.2022.127415
13. Gartner E. M., Macphee D. E. (2011): A physico-chemical basis for novel cementitious binders. *Cement and Concrete Research, 41*(7), 736-749. Doi: 10.1016/j.cemconres.2011.03.006
14. He W., Li R., Zhang Y., Nie D. (2022): Synergistic use of electrolytic manganese residue and barium slag to prepare belite-sulphoaluminate cement study. *Construction and Building Materials, 326*, 126672. Doi: 10.1016/j.conbuildmat.2022.126672
15. Ludwig H. M., Zhang W. (2015): Research review of cement clinker chemistry. *Cement and Concrete Research, 78*, 24-37. Doi: 10.1016/j.cemconres.2015.05.018
16. Chen M., Li L., Zheng Y., Zhao P., Lu L., Cheng X. (2018): Rheological and mechanical properties of admixtures modified 3D printing sulphoaluminate cementitious materials. *Construction and Building Materials, 189*, 601-611. Doi: 10.1016/j.conbuildmat.2018.09.037
17. Glasser F. P., Zhang L. (2001): High-performance cement matrices based on calcium sulfoaluminate–belite compositions. *Cement and Concrete Research, 31*(12), 1881-1886. Doi: 10.1016/S0008-8846(01)00649-4
18. Wang X., Guo M. Z., Yue G., Li Q., Ling T. C. (2022): Synthesis of high belite sulfoaluminate cement with high volume of mixed solid wastes. *Cement and Concrete Research, 158*, 10684. Doi: 10.1016/j.cemconres.2022.106845
19. Kuo W. C., Lasek J., Słowik K., Głód K., Jagustyn B., Li Y. H., Cygan A. (2019): Low-temperature pre-treatment of municipal solid waste for efficient application in combustion systems. *Energy Conversion and Management, 196*, 525-535. Doi: 10.1016/j.enconman.2019.06.007
20. Xing Z., Ping Z., Xiqiang Z., Zhanlong S., Wenlong W., Jing S., Yanpeng M. (2021): Applicability of municipal solid waste incineration (MSWI) system integrated with pre-drying or torrefaction for flue gas waste heat recovery. *Energy, 224*, 120157. Doi: 10.1016/j.energy.2021.120157
21. Yao Y., Wang W., Ge Z., Ren C., Yao X., Wu S. (2020): Hydration study and characteristic analysis of a sulfoaluminate high-performance cementitious material made with industrial solid wastes. *Cement and Concrete Composites, 112*, 103687. Doi: 10.1016/j.cemconcomp.2020.103687
22. Shi H. S., Deng K., Yuan F., Wu K. (2009): Preparation of the saving-energy sulphoaluminate cement using MSWI fly ash. *Journal of Hazardous Materials, 169*(1-3), 551-555. Doi: 10.1016/j.jhazmat.2009.03.134
23. Senff L., Castela A., Hajjaji W., Hotza D., Labrincha J. A. (2011): Formulations of sulfobelite cement through design of experiments. *Construction and Building Materials, 25*(8), 3410-3416. Doi: 10.1016/j.conbuildmat.2011.03.032
24. Wang W., Wang X., Zhu J., Wang P., Ma C. (2013): Experimental investigation and modeling of sulfoaluminate cement preparation using desulfurization gypsum and red mud. *Industrial & Engineering Chemistry Research, 52*(3), 1261-1266. Doi: 10.1021/IE301364C
25. Shen Y., Qian J., Chai J., Fan Y. (2014): Calcium sulphoaluminate cements made with phosphogypsum:

Production issues and material properties. *Cement and Concrete Composites, 48*, 67-74. Doi: 10.1016/j.cemconcomp.2014.01.009

26. Xue P., Xu A., He D., Yang Q., Liu G., Engström F., Björkman B. (2016): Research on the sintering process and characteristics of belite sulphoaluminate cement produced by BOF slag. *Construction and Building Materials, 122,* 567-576. Doi: 10.1016/j.conbuildmat.2016.06.098
27. Arjunan P., Silsbee M. R., Roy D. M. (1999): Sulfoaluminate-belite cement from low-calcium fly ash and sulfur-rich and other industrial by-products. *Cement and Concrete Research, 29*(8), 1305-1311. Doi: 10.1016/S0008-8846(99)00072-1.
28. Shen Y., Qian J., Huang Y., Yang D. (2015): Synthesis of belite sulfoaluminate-ternesite cements with phosphogypsum. *Cement and Concrete Composites, 63*, 67-75. Doi: 10.1016/j.cemconcomp.2015.09.003
29. Jansen D., Spies A., Neubauer J., Ectors D., Goetz-Neunhoeffer F. (2017): Studies on the early hydration of two modifications of ye'elimite with gypsum. *Cement and Concrete Research, 91*, 106-116. Doi: 10.1016/j.cemconres.2016.11.009
30. Iacobescu R. I., Pontikes Y., Koumpouri D., Angelopoulos G. N. (2013): Synthesis, characterization and properties of calcium ferroaluminate belite cements produced with electric arc furnace steel slag as raw material. *Cement and Concrete Composites, 44*, 1-8. Doi: 10.1016/j.cemconcomp.2013.08.002
31. Ioannou S., Reig L., Paine K., Quillin K. (2014): Properties of a ternary calcium sulfoaluminate–calcium sulfate–fly ash cement. *Cement and Concrete Research, 56*, 75-83.Doi: 10.1016/j.cemconres.2013.09.015
32. Berodier E., Scrivener K. (2015): Evolution of pore structure in blended systems. *Cement and Concrete Research, 73,* 25-35. Doi: 10.1016/j.cemconres.2015.02.025